New tools for the systematic analysis and visualization of electronic excitations. I. Formalism

Felix Plasser, Michael Wormit, and Andreas Dreuw

Citation: The Journal of Chemical Physics **141**, 024106 (2014); doi: 10.1063/1.4885819
View online: http://dx.doi.org/10.1063/1.4885819
View Table of Contents: http://scitation.aip.org/content/aip/journal/jcp/141/2?ver=pdfcov
Published by the AIP Publishing

New tools for the systematic analysis and visualization of electronic excitations. I. Formalism

Felix Plasser,[a] Michael Wormit, and Andreas Dreuw
Interdisciplinary Center for Scientific Computing, Ruprecht-Karls-University, Im Neuenheimer Feld 368, 69120 Heidelberg, Germany

(Received 15 March 2014; accepted 18 June 2014; published online 10 July 2014)

A variety of density matrix based methods for the analysis and visualization of electronic excitations are discussed and their implementation within the framework of the algebraic diagrammatic construction of the polarization propagator is reported. Their mathematical expressions are given and an extensive phenomenological discussion is provided to aid the interpretation of the results. Starting from several standard procedures, e.g., population analysis, natural orbital decomposition, and density plotting, we proceed to more advanced concepts of natural transition orbitals and attachment/detachment densities. In addition, special focus is laid on information coded in the transition density matrix and its phenomenological analysis in terms of an *electron-hole* picture. Taking advantage of both the orbital and real space representations of the density matrices, the physical information in these analysis methods is outlined, and similarities and differences between the approaches are highlighted. Moreover, new analysis tools for excited states are introduced including state averaged natural transition orbitals, which give a compact description of a number of states simultaneously, and natural difference orbitals (defined as the eigenvectors of the difference density matrix), which reveal details about orbital relaxation effects. © *2014 AIP Publishing LLC*. [http://dx.doi.org/10.1063/1.4885819]

I. INTRODUCTION

An immense increase in computational power and continually improving methodology have extended the scope of quantum chemical computations of excited states to ever larger system sizes.[1–3] However, these improvements pose new challenges for analysis, not only in the context of quick and automated processing of the results, but even more with respect to understanding correlation and relaxation phenomena, some of which only come into play at extended system sizes. A complete comprehension of all the relevant processes is particularly challenging in the field of molecular electronics where concepts from quantum chemistry and solid state physics have to be combined to describe the properties of the system under study. But there are also many other areas of computational quantum chemistry which may benefit significantly from advanced analysis methods (e.g., when creating a parameterized model or assessing the reliability of a computational protocol).

In light of these considerations, we implemented a general suite for excited state analysis in the framework of the *ab initio* algebraic diagrammatic construction (ADC) scheme of the polarization propagator[4] (considering the different variants of this method up to third order in many-body perturbation theory). The presented toolbox integrates a number of previously published approaches, but also provides several new ideas. It is built around the concepts of (i) natural orbitals (NOs),[5] (ii) natural transition orbitals (NTOs),[6–8] (iii) the attachment/detachment analysis of the difference density matrix,[9] and (iv) a decomposition of the one-particle transition density matrix (1TDM) to analyze charge resonance and excitonic correlation phenomena.[10] Whereas the first three methods are in common use, the fourth one has been introduced recently by some of us, following previous work,[11–15] and only a preliminary implementation has been made available so far.[10] However, also the potential of this latter methodology has already been exploited by a number of researchers studying organic electronics and photobiology.[16–20] A unified formalism is present through the use of one-particle density matrices (1DM) and transition density matrices, a common ground, which allows for a clear comparison between the different methods and suggests extensions leading to a wide variety of routines for population analysis, as well as, orbital and density plotting, which are provided in this implementation. To our knowledge, a similarly comprehensive analysis toolbox has not been made available so far, let alone in a correlated *ab initio* framework. Therefore, this implementation carries great potential to provide unprecedented insight into excited states of molecular systems.

The purpose of this work is to provide a solid theoretical foundation for the application of this new analysis suite, by showing the precise equations implemented and discussing the underlying physics in detail. In particular, an analysis of the 1TDM, which we introduced in Ref. 10, will be reiterated using the *electron-hole* pair representation of the excited state. This interpretation will be supported with arguments from Green's function theory. In Paper II,[21] a preview of the power of these methods will be provided through a number of practi-

[a]Electronic mail: felix.plasser@iwr.uni-heidelberg.de. URL: http://www.iwr.uni-heidelberg.de/groups/compchem/.

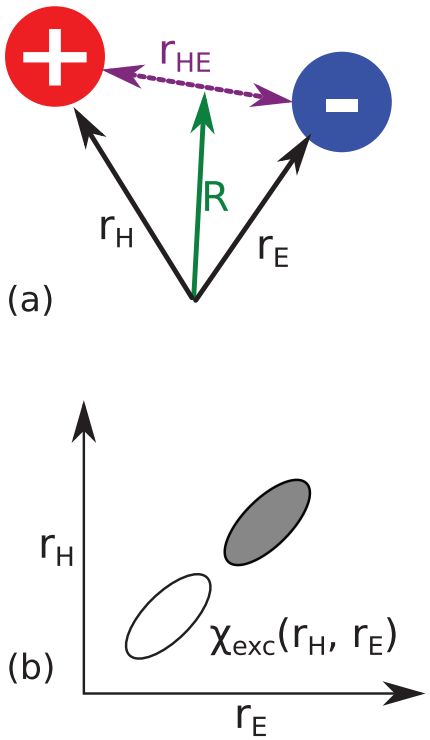

FIG. 1. The *electron-hole* representation of an electronic excitation: (a) the *hole* and *electron* coordinates r_H and r_E, the center-of-mass coordinate R, and the separation r_{HE}, and (b) an exemplary wavefunction $\chi_{exc}(r_H, r_E)$.

cal examples. First, a focus will be put on differences between the eigenvectors of the difference density matrix (natural difference orbitals, NDOs) and the NTOs (as computed from the 1TDM), and it will be shown that these derive from orbital relaxation effects. Second, the use of state-averaged NTOs (SA-NTOs) for the compact simultaneous representation of a number of excited states will be illustrated. Furthermore, the analysis of charge resonance effects will be discussed, and the potential of our methods in the case of doubly excited states and unrestricted references will be highlighted.

Before going into the more technical part of this work, we want to start our discussion by mentioning that there are two opposing strategies relevant to the description of excited states. For small molecules, it is typical to consider the occupied (*hole*) and virtual (*particle*) orbitals involved in an excitation independently ("quantum chemistry" picture). Based on the shape of these orbitals, states are classified according to their character, e.g., $n\pi^*$, $\pi\pi^*$, $\pi\sigma^*$. An entirely different point of view ("solid state physics") is usually taken in the case of extended or periodic systems. In such cases, the excited state is viewed as a quasi-particle (exciton), whose internal structure is determined by the *electron-hole* separation and the exciton binding energy.[22,23] The two views can be reconciled when considering an underlying two-body wavefunction of the exciton. This idea is illustrated in Fig. 1: the exciton is considered as consisting of two particles, a *hole* and an (excess) *electron* positioned at the coordinates r_H and r_E, respectively, whose correlated motion is described by the wavefunction $\chi_{exc}(r_H, r_E)$. Such a wavefunction arises naturally out of the electron-hole response function, which is governed by the Bethe-Salpeter equation.[24–26] Using arguments

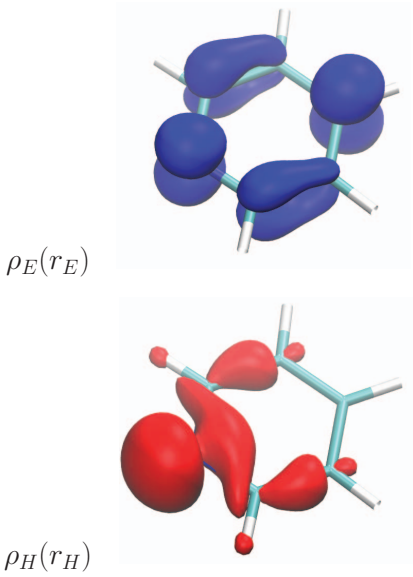

FIG. 2. Deconstruction of the exciton wavefunction $\chi_{exc}(r_H, r_E)$ into separate *hole* $\rho_H(r_H)$ and *particle* $\rho_E(r_E)$ densities, using an $n\pi^*$ excited state in pyridine as example.

from Green's function theory, we will point out that for many-body quantum chemical computations the 1TDM between the ground and excited state γ^{0I} can be identified with this wavefunction.

Starting with χ_{exc} the "quantum chemistry" picture may be restored by realizing that in the case of small molecules the *electron* and *hole* motions are approximately uncorrelated.[27] Then it is meaningful to construct an attachment/detachment representation by integrating over one of the respective coordinates. For this purpose, one defines a *hole* density

$$\rho_H(r_H) = \int \chi_{exc}(r_H, r_E)^2 \, dr_E \tag{1}$$

as well as a *particle* (or excess electron) density

$$\rho_E(r_E) = \int \chi_{exc}(r_H, r_E)^2 \, dr_H \tag{2}$$

as shown in Fig. 2.

The "solid state physics" picture arises from an entirely different assumption. The coordinate system is transformed into the center-of-mass $R = (r_H + r_E)/2$ and *electron-hole* separation $r_{HE} = r_E - r_H$ coordinates (cf. Fig. 1). And the wavefunction is factorized in terms of these coordinates[28]

$$\chi_{exc}(r_H, r_E) = \phi_{CM}(R)\phi_{sep}(r_{HE}). \tag{3}$$

This situation is depicted in Fig. 3: ϕ_{CM} may be modelled as a particle-in-a-box wavefunction[27] or more generally, using exciton scattering theory.[29] ϕ_{sep}, on the other hand, should behave like a hydrogen atom,[23,30] only that dielectric screening has to be taken into account and an effective mass has to be assigned.

Molecules with extended π-systems occupy an intermediate position between these two extremes.[17,23] While the "quantum chemistry" picture is certainly able to provide a large amount of insight for these systems, there are some pieces of information which are invariably lost, when the *elec-*

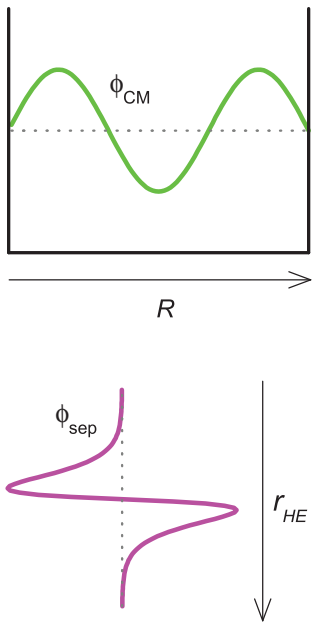

FIG. 3. Deconstruction of the exciton wavefunction $\chi_{exc}(r_H, r_E)$ into a center-of-mass $\phi_{CM}(R)$ and an *electron-hole* separation $\phi_{sep}(r_{HE})$ component.

tron and *hole* are viewed independently. *Electron-hole* correlations are the very property distinguishing excitons from free charge carriers, and their extent is the key difference between strongly bound Frenkel excitons and weakly bound Wannier excitons.[25] Understanding such properties is not only of academic interest but also has high relevance for solar cell design.[31] Furthermore, there is an important methodological component of this issue, which has been observed in many cases of molecules with large π-systems:[32–36] dynamic *electron-hole* separation impacts the quality of time-dependent density functional computations in a very similar sense as static directed charge transfer[37] does, and the outcome has been described as being a source of "significant but hard-to-detect errors."[38] The occurrence of charge resonance states in molecular dimers and aggregates[10,11,39,40] is a related phenomenon which is difficult to understand in the "quantum chemistry" picture.

Aside from this fundamental problem of *electron-hole* correlations, there are a number of other wavefunction properties which are difficult to understand in the standard orbital excitation picture. These are in particular concerned with electron correlation and relaxation effects. Moreover, it is in many cases highly desirable to have quick and automated analysis methods. We will present strategies addressing all these issues.

II. NOTATION

To denote orbital indices, we will use subscripts and differentiate between three different types:

- μ, ν, ξ, ζ: atomic orbitals (AO) $\chi_\mu(r)$ (these equations hold for any, possibly non-orthogonal, basis set; some equations use the fact that the AOs are atom-centered).
- p, q, r, s: molecular orbitals (MO) $\phi_p(r)$ (these are only required to be orthonormal). Density matrices expressed within the MO basis are marked with a tilde: $\tilde{\mathbf{D}}^{IJ}$.
- i, j: orbitals $\psi_i^{IJ}(r)$ specifically computed using the methods described later in this work: NOs and NTOs.

Creation (annihilation) operators with respect to these orbitals are written as $\hat{a}_\mu^\dagger$ ($\hat{a}_\nu$), etc.

Superscripts I, J are used to index electronic states, e.g., Ψ^I. A superscript 0 will be used to refer specifically to the ground state. In some cases (e.g., transformation matrices and population numbers), these superscripts are dropped for notational brevity.

Most expressions will be written in their general form, which is the spin-orbital basis. Further spin-dependent manipulations (i.e., considering the separate α and β, spin-traced or spin-difference density matrices), are straightforward and will only be considered in this text when necessary. For simplicity, it will be assumed that all orbitals and coefficients are real. However, the expressions may be readily extended to complex numbers.

III. GENERAL CONSIDERATIONS

We consider the general case of solving the Schrödinger equation of an n-electron system. The ground state is given as the eigenfunction with the lowest energy eigenvalue E^0 determined as

$$\hat{H}\Psi^0(r_1, \ldots, r_n) = E^0\Psi^0(r_1, \ldots, r_n), \tag{4}$$

where r_i denotes the vector of spatial and spin coordinates of the ith electron. And any excited state I may be (at least formally) constructed as

$$\hat{H}\Psi^I(r_1, \ldots, r_n) = E^I\Psi^I(r_1, \ldots, r_n), \tag{5}$$

where $E^I > E^0$. In general, Ψ^0 and Ψ^I are many-particle functions that may differ in any possible way. In many cases, however, it is possible to view the electronic excitation in terms of only a few orbital substitutions. For this purpose, it is instructive to consider an underlying spin-orbital basis and construct

$$\Psi^I = \left(\sum_{\mu\nu} C^I_{\mu\nu}\hat{a}^\dagger_\mu\hat{a}_\nu + \sum_{\mu\nu\xi\zeta} C^I_{\mu\nu\xi\zeta}\hat{a}^\dagger_\xi\hat{a}^\dagger_\mu\hat{a}_\nu\hat{a}_\zeta + \cdots\right)\Psi^0. \tag{6}$$

Such a construction is certainly possible when both Ψ^0 and Ψ^I are elements of the n-particle Hilbert space constructed from the orbital basis and when all relevant substitutions are included in the summation.[41] For the phenomenological understanding of this equation it is instructive to consider Ψ^0 as an inactive reference state or as the "Fermi-vacuum" (see, e.g., Refs. 15 and 42). Then, Ψ^I can be seen as being constructed of *holes* and (excess) *electrons* (or *particles*) in this Fermi-vacuum, which correspond to the annihilation and creation operators, respectively. In other words, these operators show how electrons have to be shifted in Ψ^0 to obtain Ψ^I (cf. Fig. 4). Depending on the number of successive

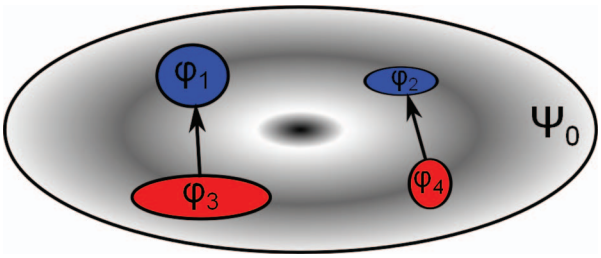

FIG. 4. The *electron-hole* pair representation of an electronic excitation (using the example of Ψ^1 of Eq. (7)): rather than analyzing the excited state wavefunction directly, one considers electron shifts with respect to the ground state Ψ^0.

annihilations and creations, states are classified as singly excited, doubly excited, etc.

Equation (6) may be used to illustrate two additional concepts relevant to the discussions in this paper. First, the specific values of the $C^I_{\mu\nu}, C^I_{\mu\nu\xi\zeta}, \ldots$ coefficients will depend on the orbital basis chosen. According to the choice of orbitals, the excitation character may be more or less clearly visible. Second, *electrons* and *holes* are never created individually, but in correlated pairs (or quadruples, etc.). This idea can be illustrated by considering that the wavefunctions

$$\Psi^1 = 2^{-1/2}\left(\hat{a}_1^\dagger \hat{a}_3 + \hat{a}_2^\dagger \hat{a}_4\right)\Psi^0, \tag{7}$$

$$\Psi^2 = 2^{-1/2}\left(\hat{a}_1^\dagger \hat{a}_4 + \hat{a}_2^\dagger \hat{a}_3\right)\Psi^0, \tag{8}$$

are obviously different, even though they may possess the same overall *hole* and (excess) *electron* densities. These differences may be termed *electron-hole* correlations, a phenomenon which is closely connected to the static correlation of the excited state (see below and Ref. 15).

Equation (6) cannot be directly used for the analysis of excited states, as some terms may be ill defined (i.e., a $C^I_{\mu\nu}$ coefficient where either ν is very weakly or μ is very strongly occupied). However, there is a closely related concept in quantum chemistry, which is suitable for this purpose: reduced (transition) density matrices. Given two states, indexed I and J, an element of the 1TDM between them is constructed as

$$D^{IJ}_{\mu\nu} = \langle \Psi^I | \hat{a}_\mu^\dagger \hat{a}_\nu | \Psi^J \rangle, \tag{9}$$

where μ and ν are two orbital indices. A state density matrix (1DM) $\mathbf{D}^{II}$ is obtained in the case of $I = J$. Reduced density matrices are important quantities as they are directly related to the matrix elements of one-particle operators. For a one-particle operator $\hat{O}_1$, it holds that the associated (transition) property is given as

$$\langle \Psi^I | \hat{O}_1 | \Psi^J \rangle = \sum_{\mu\nu} D^{IJ}_{\mu\nu} \langle \chi_\mu | \hat{O}_1 | \chi_\nu \rangle, \tag{10}$$

i.e., all necessary wavefunction dependent information is already contained in the 1TDM.

Revisiting Eq. (6) it may be seen that in the case of a single determinant ground state Ψ^0, the 1TDM elements directly give the coefficient as defined in the expansion (i.e., $C^I_{\mu\nu} = D^{0I}_{\nu\mu}$, see also Ref. 43). For general wavefunctions, we argue that the 1TDM is a more natural way to define single excitation coefficients, as opposed to the $C^I_{\mu\nu}$, owing to its direct connection to physical observables (see Eq. (10)) and other favorable properties (see below).

For the purpose of visualization, it is helpful to express the 1TDM in coordinate space (see, e.g., Refs. 44 and 45)

$$\gamma^{IJ}(r, r') = n \int \Psi^I(r, r_2, \ldots, r_n)\Psi^J(r', r_2, \ldots, r_n) dr_2 \ldots dr_n, \tag{11}$$

where the integration is performed over all coordinates except for the first one. The connection to Eq. (9) is

$$\gamma^{IJ}(r, r') = \sum_{\mu\nu} D^{IJ}_{\mu\nu} \chi_\mu(r) \chi_\nu(r'). \tag{12}$$

If $\hat{O}_1$ is given as a sum of operators acting on the individual n electrons, i.e.,

$$\hat{O}_1 = \sum_{i=1}^{n} \hat{o}(r_i), \tag{13}$$

then Eq. (10) may be reexpressed in coordinate space

$$\langle \Psi^I | \hat{O}_1 | \Psi^J \rangle = \iint \delta(r - r') \hat{o}(r') \gamma^{IJ}(r, r') dr dr', \tag{14}$$

where $\delta(r - r')$ is the Dirac-δ function. With this definition the origin of the prefactor n in Eq. (11) becomes apparent: it replaces the summation over the n individual electrons of Eq. (13).

If the operator does not explicitly act on r' (i.e., $\hat{o}(r') = f(r')$), which is, for example, the case when computing multipole moments, then Eq. (14) is simplified to

$$\int \left(\int \delta(r - r') \gamma^{IJ}(r, r') dr \right) f(r') dr' = \int f(r') \gamma^{IJ}(r', r') dr' = \int f(r) \rho^{IJ}(r) dr. \tag{15}$$

In other words, the integration is performed over the density rather than the density matrix.

IV. STATE DENSITY MATRICES

State density matrices, i.e., expressions of the type

$$\gamma^{II}(r, r') = n \int \Psi^I(r, r_2, \ldots, r_n)\Psi^I(r', r_2, \ldots, r_n) dr_2 \ldots dr_n$$

give rise to some of the most widely used concepts in quantum chemistry. There are three main types of analysis methods, which will reappear in a very similar form also for the transition and difference density matrices: (i) plotting the density, (ii) population analysis, and (iii) diagonalization of the density matrix. For plotting one may use the total electron density, which is defined as the diagonal part of the density matrix

$$\rho^{II}(r) = \gamma^{II}(r, r). \tag{16}$$

For every point r in space it holds that $\rho^{II}(r) \geq 0$ and the integral over all space equals the number of electrons

$$\int \rho^{II}(r) dr = n. \tag{17}$$

Inserting the orbital representation (Eq. (12)) this may be rewritten as

$$n = \int \sum_{\mu\nu} D^{II}_{\mu\nu} \chi_\mu(r)\chi_\nu(r)dr$$
$$= \sum_{\mu\nu} D^{II}_{\mu\nu} S_{\mu\nu} = \mathrm{Tr}(\mathbf{D}^{II}\mathbf{S}), \quad (18)$$

where the overlap matrix $\mathbf{S}$ was defined as

$$S_{\mu\nu} = \int \chi_\mu(r)\chi_\nu(r)dr. \quad (19)$$

A. Population analysis

The objective of a population analysis is to partition Eq. (17) into individual atomic contributions. Formally, one may define the (gross) population number of atom A in state I

$$n^I(A) = \int_A \rho^{II}(r)dr \quad (20)$$

as the integral of the density over the space belonging to this atom. The net charge of the atom

$$c^I(A) = z(A) - n^I(A) \quad (21)$$

is obtained by subtracting this number from the nuclear charge $z(A)$.

To evaluate Eq. (20) in orbital space, one may use Eq. (12) to obtain

$$n^I(A) = \sum_{\mu\nu} D^{II}_{\mu\nu} \int_A \chi_\mu(r)\chi_\nu(r)dr = \sum_{\mu\nu} D^{II}_{\mu\nu} S^{(A)}_{\mu\nu}, \quad (22)$$

where the symbol $S^{(A)}_{\mu\nu}$ is used to refer to the partial overlap integral between χ_μ and χ_ν counting only the contribution on atom A. From this expression, one may derive the Mulliken analysis scheme[46] by using an AO basis and partitioning the overlap matrix elements in dependence of the atom on which they are situated, i.e.,

$$S^{(A)}_{\mu\nu} = \begin{cases} S_{\mu\nu} & : \quad \mu,\nu \in A \\ \frac{1}{2}S_{\mu\nu} & : \mu \in A, \nu \notin A \\ \frac{1}{2}S_{\mu\nu} & : \mu \notin A, \nu \in A \\ 0 & : \quad \text{else} \end{cases}, \quad (23)$$

where $\mu \in A$ means that χ_μ is an AO situated on atom A etc. Then Eq. (22) becomes

$$n^I(A) = \sum_{\mu\in A}\sum_{\nu\in A} D^{II}_{\mu\nu} S_{\mu\nu}$$
$$+\frac{1}{2}\sum_{\mu\in A}\sum_{\xi\notin A} D^{II}_{\mu\xi} S_{\mu\xi} + \frac{1}{2}\sum_{\xi\notin A}\sum_{\nu\in A} D^{II}_{\xi\nu} S_{\xi\nu}. \quad (24)$$

Since the matrices $\mathbf{D}^{II}$ and $\mathbf{S}$ are symmetric, the sums can be rearranged to yield a more compact expression

$$n^I(A) = \sum_{\mu\in A}\sum_{\zeta} D^{II}_{\mu\zeta} S_{\mu\zeta} = \sum_{\mu\in A} (\mathbf{D}^{II}\mathbf{S})_{\mu\mu}. \quad (25)$$

In the current paper, only Mulliken style population analysis will be considered. But it is certainly possible to extend such concepts as presented here to the Löwdin or other types of population analysis (see also Refs. 38 and 47).

B. Natural orbitals

Considering that a state density matrix is symmetric, it may be diagonalized using an orthogonal matrix. For this purpose, one considers the matrix representation $\tilde{\mathbf{D}}^{II}$ with respect to an orthonormal (e.g., MO) basis and diagonalizes it using an orthogonal matrix $\mathbf{T}$

$$\mathbf{T}^{\mathrm{T}}\tilde{\mathbf{D}}^{II}\mathbf{T} = \mathrm{diag}(n_1, n_2, \ldots). \quad (26)$$

The n_i are interpreted as the occupation numbers of the natural orbitals. According to Eq. (18) the sum of the occupation numbers is identical to the number of electrons n

$$n = \sum_i n_i. \quad (27)$$

The NOs ψ^{II}_i are defined by the columns of the $\mathbf{T}$-matrix

$$\psi^{II}_i(r) = \sum_p T_{pi}\phi_p(r). \quad (28)$$

In terms of the NOs, the density matrix can be expressed in diagonal form by transforming Eq. (12) (see Appendix A)

$$\gamma^{II}(r,r') = \sum_i n_i \psi^{II}_i(r)\psi^{II}_i(r'). \quad (29)$$

And the density is of course just the weighted sum over squared NOs

$$\rho^{II}(r) = \sum_i n_i \left(\psi^{II}_i(r)\right)^2. \quad (30)$$

The NO occupation numbers may be used for a meaningful description of the number of unpaired electrons.[48,49] For this purpose, it is most instructive to use the spin-averaged occupation numbers pertaining to spatial orbitals $\bar{n}_i$ ($0 \le \bar{n}_i \le 2$). In a restricted Hartree-Fock wavefunction, all $\bar{n}_i$ are either zero or two. Any deviation from this distribution may therefore be termed "electron correlation." There is, however, no unique way to quantify this deviation and a number of ideas have been suggested (see, e.g., Refs. 48 and 49). In our implementation, two different formulae are considered, a linear one

$$n_u = \sum_i \min(\bar{n}_i, 2 - \bar{n}_i) \quad (31)$$

and a nonlinear one

$$n_{u,nl} = \sum_i \bar{n}_i^2 (2 - \bar{n}_i)^2 \quad (32)$$

(both taken from Ref. 49). The n_u value is intended to count all types of correlation, i.e., dynamical (deriving from a large number of small $\bar{n}_i$ values) and static (deriving from a small number of large $\bar{n}_i$ values). $n_{u,nl}$, on the other hand, is aimed at suppressing contributions from dynamical correlation, highlighting static correlation and radical character. Therefore, this second measure could be applied successfully to analyze radical character in large systems.[50,51]

V. TRANSITION DENSITY MATRICES

An analysis of the 1TDM has been introduced recently,[10] which enables the identification of charge resonance and excitonic correlation effects in quantum chemical calculations, following previous work by other researchers.[11–15] While our initial work[10] was based on phenomenological reasoning, a more solid foundation of this approach will be given here. It will first be shown that the 1TDM corresponds to the *electron-hole* amplitudes χ_{exc} (Fig. 1) as defined within the polarization propagator of the *electron-hole* response function (see also Ref. 52). Subsequently, this identification will be used to derive equations for a number of different properties of the *electron-hole* pair. It may be mentioned here that the 1TDM can of course be readily used to analyze the properties of the *electron* and *hole* independently. But, more importantly, it also encodes two-particle correlation effects, which are difficult to examine otherwise. Both types of properties will be discussed in this chapter.

A. Discussion of the polarization propagator

Our discussion starts with the *electron-hole* response function

$$L(1,2;1',2') = G_2(1,2;1',2') - G_1(1,1')G_1(2,2') \quad (33)$$

which is the central entity for the excitation problem within the framework of many-body Green's functions.[53,54] Here, each set of variables (1) comprises position and spin, and time coordinates $(1) = (r_1, t_1)$. $G_1(1, 1')$ and $G_2(1, 2; 1', 2')$ refer to the one- and two-particle Green's function, respectively, which are defined as

$$G_1(1,1') = -\imath \langle \Psi_0 | \hat{T}\left[\hat{\psi}_H(1)\hat{\psi}_H^\dagger(1')\right]|\Psi_0\rangle, \quad (34)$$

$$G_2(1,2;1',2') = (-\imath)^2 \langle \Psi_0 | \hat{T}\left[\hat{\psi}_H(1)\hat{\psi}_H(2)\hat{\psi}_H^\dagger(2')\hat{\psi}_H^\dagger(1')\right]|\Psi_0\rangle, \quad (35)$$

where $\hat{T}$ is the time-ordering operator, while $\hat{\psi}_H^\dagger(1)$ and $\hat{\psi}_H(1)$ are the field operators in the Heisenberg picture. In Eq. (33), it can be seen that the *electron-hole* response function depends on four time variables. For optical excitations, however, the physical information is already contained in the simpler polarization propagator

$$\Pi(r_1, r_1'; r_2', r_2; t, t') = \lim_{\substack{t_1, t_1' \to t \\ t_2, t_2' \to t'}} \imath L(1,2;1',2') \quad (36)$$

which only depends on two time variables (simultaneous excitation and de-excitation). Furthermore, in case of time-independent Hamiltonians only the time difference between the two variables is relevant. The one-dimensional Fourier transform then yields the spectral representation of the polarization propagator

$$\Pi(r_1, r_1'; r_2', r_2; \omega) = \sum_{I \neq 0} \left[\frac{\chi^I(r_2, r_2')\chi^{I*}(r_1', r_1)}{\omega + (E^I - E^0)} - \frac{\chi^I(r_1, r_1')\chi^{I*}(r_2', r_2)}{\omega - (E^I - E^0)} \right] \quad (37)$$

which possesses poles at the excitation energies. The residuals to these poles are comprised of the electron-hole amplitudes $\chi^I(r, r')$ which have the form

$$\chi^I(r, r') = \langle \Psi^0 | \hat{\psi}^\dagger(r')\hat{\psi}(r) | \Psi^I \rangle = \chi^I_{exc}(r, r'), \quad (38)$$

where $\hat{\psi}^\dagger(r)$ and $\hat{\psi}(r)$ are the usual field operators in the Schrödinger picture. These field operators may now be expanded in terms of creation and annihilation operators of single-particle orbitals

$$\hat{\psi}(r) = \sum_p \phi_p(r)\hat{a}_p \text{ and } \hat{\psi}^\dagger(r) = \sum_p \phi_p^*(r)\hat{a}_p^\dagger.$$

Using this form, we can directly identify the *electron-hole* amplitudes with the 1TDM as given in Eq. (12)

$$\chi^I_{exc}(r_H, r_E) = \sum_{pq} \phi_p^*(r_H) \underbrace{\langle \Psi_0 | \hat{a}_p^\dagger \hat{a}_q | \Psi_I \rangle}_{=D^{0I}_{pq}} \phi_q(r_E) = \gamma^{0I}(r_H, r_E). \quad (39)$$

Equation (39) provides a well-defined starting point for further analysis of χ_{exc}, which will be done in detail below. The meaning of this identification is also quite apparent: $\hat{a}_q$ annihilates the *electron* in orbital ϕ_q while $\hat{a}_p^\dagger$ creates the hole in ϕ_p.

Finally, we want to discuss the special case where Ψ^0 is dominated by a single determinant. In such a case, the 1TDM elements may be directly identified with the excitation operators transforming Ψ^0 into Ψ^I (cf. Eq. (6)). In particular, for a configuration interaction wavefunction with single excitations (CIS) the 1TDM is identical to the CI-vector. If $c_p^{q,I}$ marks the CI-coefficient of the configuration where an electron was promoted from MO ϕ_p to ϕ_q, then according to the Slater-Condon rules

$$\tilde{D}^{0I}_{pq} = c_p^{q,I}. \quad (40)$$

Such a relation does not exist for more extended wavefunction models. However, to help with a qualitative interpretation of the results, we want to point out that in many cases the 1TDM elements are indeed of similar magnitude as the corresponding elements of the response vector.

B. Transition densities

The transition density ρ^{0I} is defined as the diagonal part of the transition density matrix

$$\rho^{0I}(r) = \gamma^{0I}(r, r). \quad (41)$$

In the *electron-hole* picture, the square of $\rho^{0I}(r)$ measures the probability that the *electron* and *hole* are simultaneously at a location $r = r_H = r_E$. In this context, it should be pointed out that the transition density vanishes whenever $r_H \neq r_E$, e.g., it disappears in the case of completely charge separated states. ρ^{0I} contains areas of positive and negative sign. The integral over all space is zero as can be seen by inserting Eq. (11) (and considering orthogonal wavefunctions)

$$\int \rho^{0I}(r)dr = 0 \; (I \neq 0). \quad (42)$$

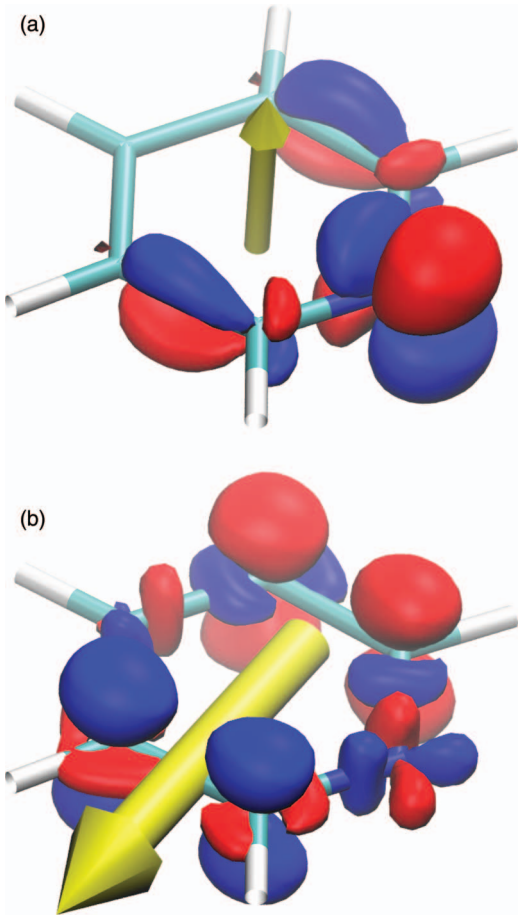

FIG. 5. Comparison of transition densities (shown as plots with isovalue 0.007 e) and transition dipole moments (shown as yellow arrows with volume proportional to the oscillator strength) in the case of an $n\pi^*$ (1^1B_2) (a) and a $\pi\pi^*$ (2^1B_1) (b) state of pyridine.

Higher multipole moments of this distribution are the decisive quantities determining the interaction strength of an electronic transition with light and the efficiency of excitation energy transfer. In particular, the transition dipole moment

$$\vec{\mu} = \langle \Psi^0 | \vec{r} | \Psi^I \rangle = \int \vec{r}\, \rho^{0I}(r) dr \tag{43}$$

is usually considered for this purpose (see also Eq. (15)). Here, $\vec{r}$ refers to a vector containing the three spatial coordinates. The connection between the transition densities and moments is illustrated in Fig. 5. In this representation, it can be seen that the transition dipole moment is a vector pointing toward the positive (blue) part of the transition density.

C. Hole and particle densities

Using γ^{0I} for χ_{exc} and inserting Eq. (12) into Eq. (1) gives the following equation for the *hole* density:

$$\rho_H(r_H) = \int \gamma^{0I}(r_H, r_E)^2 dr_E = \sum_{\mu\nu} [\mathbf{D}^{0I}\mathbf{S}(\mathbf{D}^{0I})^{\mathrm{T}}]_{\mu\nu}\, \chi_\mu(r_H)\chi_\nu(r_H). \tag{44}$$

And analogously from Eq. (2) one obtains

$$\rho_E(r_E) = \int \gamma^{0I}(r_H, r_E)^2 dr_H = \sum_{\mu\nu} [(\mathbf{D}^{0I})^{\mathrm{T}}\mathbf{S}\mathbf{D}^{0I}]_{\mu\nu}\, \chi_\mu(r_E)\chi_\nu(r_E). \tag{45}$$

These densities (see also Ref. 55) will be termed the *hole/particle* densities. They bear resemblance to the attachment/detachment densities discussed below with the difference that the latter also include higher excitation and relaxation effects. Example plots of these densities are presented in Fig. 2. In addition to visual inspection, these densities have also been subjected to population analysis.[38,56]

When integrating ρ_H and ρ_E over all space, one obtains a central quantity of our analysis scheme

$$\Omega = \int \rho_H(r_H) dr_H = \int \rho_E(r_E) dr_E = \iint \gamma^{0I}(r_H, r_E)^2 dr_E dr_H. \tag{46}$$

After insertion of Eq. (12) one obtains (in the general case of a non-orthogonal orbital basis set)

$$\Omega = \sum_{\mu\nu} (\mathbf{D}^{0I}\mathbf{S})_{\mu\nu} (\mathbf{S}\mathbf{D}^{0I})_{\mu\nu} = \mathrm{Tr}((\mathbf{D}^{0I})^{\mathrm{T}}\mathbf{S}\mathbf{D}^{0I}\mathbf{S}), \tag{47}$$

an expression, which was initially introduced with a somewhat more heuristic reasoning.[10] In the case of an orthogonal (e.g., MO) basis, Ω is the squared Frobenius norm of the $\tilde{\mathbf{D}}^{0I}$ matrix (cf. Refs. 40 and 45). Equation (47) is a natural extension of this concept providing an expression, which is invariant to any basis set transformation. In the case of CIS, considering a MO basis (where $\mathbf{S}$ becomes a unit matrix) and using Eq. (40), it can clearly be seen that

$$\Omega_{\mathrm{CIS}} = \sum_{p,q} \left(c_p^{q,I}\right)^2 = 1 \tag{48}$$

in the case of a normalized wavefunction.[57] For other wavefunction models than CIS, Ω may be considered as a measure for the amount of single excitation character (see also Ref. 20). It has been pointed out that Ω may be used for a rough estimation of the coupling matrix element with respect to a one-electron operator $\hat{O}$ (cf. Eq. (10)).[40] This is true in the sense that from $\Omega = 0$ it rigorously follows that $\langle \Psi^0 | \hat{O} | \Psi^I \rangle = 0$. However, $\Omega \approx 1$ is certainly not a sufficient condition for a large coupling matrix element. Considering, for example, transition moments such a heuristic does correctly identify doubly excited states as being optically forbidden. However, other classes of optically forbidden transitions (e.g., due to charge transfer character or symmetry reasons) cannot be identified in such a simple way.

D. Charge transfer numbers

An analysis of the electron-hole distribution may be achieved by partitioning Ω into contributions deriving from different pairs of atoms[57] or general molecular fragments[10] leading to the so-called charge transfer numbers. In real space, the charge transfer number from fragment A to fragment B

may be defined as

$$\Omega_{AB} = \int_A \int_B \gamma^{0I}(r_H, r_E)^2 dr_E dr_H, \tag{49}$$

where the integrations go over the volume elements pertaining to A and B, respectively. Ω_{AB} is the probability of finding the *hole* on fragment A while the *electron* is on fragment B. To represent the charge transfer numbers in orbital space, it is necessary to partition Eq. (47) into atomic contributions. We have previously suggested[10] using the expression

$$\Omega_{AB} = \sum_{\mu \in A} \sum_{\nu \in B} (\mathbf{D}^{0I}\mathbf{S})_{\mu\nu} (\mathbf{S}\mathbf{D}^{0I})_{\mu\nu} \tag{50}$$

which is analogous to Mayer's bond order.[58] However, a more detailed consideration leads to the somewhat altered formula

$$\Omega_{AB} = \frac{1}{2} \sum_{\mu \in A} \sum_{\nu \in B} \left[(\mathbf{D}^{0I}\mathbf{S})_{\mu\nu} (\mathbf{S}\mathbf{D}^{0I})_{\mu\nu} + D^{0I}_{\mu\nu} (\mathbf{S}\mathbf{D}^{0I}\mathbf{S})_{\mu\nu} \right] \tag{51}$$

which is derived by inserting Eq. (12) into Eq. (49) and using Eq. (23), see Appendix B. This corrected formula is used in the current implementation. Both formulae provide a partitioning of the total Ω value in the sense that

$$\sum_{A,B} \Omega_{AB} = \Omega. \tag{52}$$

As one option, the Ω_{AB} (or related data) may be visualized directly, yielding what has been termed an *electron-hole* pair correlation plot.[12,59,60] Alternatively, the information may be contracted further to yield different statistical descriptors representing charge transfer, delocalization, etc.[10,12] This analysis proved to be helpful, e.g., for studying the structure of excitons in conjugated organic polymers[17] and for quantifying delocalization and charge transfer effects in DNA base stacks.[16,20] Furthermore, the effect of charge resonance interactions on the formation of excimers was highlighted using this approach.[10,61,62]

E. Natural transition orbitals

A simple diagonalization of the transition density matrix as in the case of a state density matrix is not generally possible, since it is non-symmetric. However, it is instructive to perform a singular value (SV) decomposition, which leads to the NTOs[6–8]

$$\tilde{\mathbf{D}}^{0I} = \mathbf{U}\ \mathrm{diag}(\sqrt{\lambda_1}, \sqrt{\lambda_2}, \ldots)\mathbf{V}^{\mathrm{T}}. \tag{53}$$

An equivalent way to define the NTOs is by stating that the unitary $\mathbf{U}$ and $\mathbf{V}$ matrices contain the eigenvectors of the *hole* $\tilde{\mathbf{D}}^{0I}\tilde{\mathbf{D}}^{0I,\mathrm{T}}$ and *particle* $\tilde{\mathbf{D}}^{0I,\mathrm{T}}\tilde{\mathbf{D}}^{0I}$ matrices, respectively (cf. Eqs. (44) and (45)).[7] The $\mathbf{U}$ matrix is used to construct the *hole* NTOs

$$\psi_i^{0I}(r) = \sum_p U_{pi} \phi_p(r) \tag{54}$$

while the $\mathbf{V}$ matrix defines the *particle* NTOs

$$\psi_i^{I0}(r) = \sum_p V_{pi} \phi_p(r). \tag{55}$$

The weights of the respective configurations are represented by the λ_i. In analogy to Eq. (29), the 1TDM can be represented in terms of the NTOs (see Appendix A and Ref. 15)

$$\gamma^{0I}(r, r') = \sum_i \sqrt{\lambda_i} \psi_i^{0I}(r) \psi_i^{I0}(r'). \tag{56}$$

In a similar fashion, one may express the *hole* and *particle* densities

$$\rho_H(r_H) = \sum_i \lambda_i \left(\psi_i^{0I}(r_H)\right)^2, \tag{57}$$

$$\rho_E(r_E) = \sum_i \lambda_i \left(\psi_i^{I0}(r_E)\right)^2, \tag{58}$$

in diagonal form by using the NTOs.

Usually only one or two of the λ_i differ significantly from 1, which allows a compact representation of the electronic excitation. NTOs are therefore of great use in cases where the canonical Hartree-Fock orbitals do not provide such a compact description. There is a subtle but important meaning contained in the number of non-zero SVs, a feature, which will be quantified using the NTO participation ratio

$$\mathrm{PR}_{\mathrm{NTO}} = \frac{\left(\sum_i \lambda_i\right)^2}{\sum_i \lambda_i^2} = \frac{\Omega}{\sum_i \lambda_i^2}. \tag{59}$$

$\mathrm{PR}_{\mathrm{NTO}}$ gives the number of independent contributions needed to describe the excitation. An analogous quantity has been termed "collectivity index," which was related to entropy.[13,55] A CIS state with $\mathrm{PR}_{\mathrm{NTO}} = 1$ can be expressed by a single configuration state function, whereas in the case of $\mathrm{PR}_{\mathrm{NTO}} > 1$ several configurations are needed to describe the excited state, which can be identified with static electron correlation.[15] More specifically, it has been pointed out that in the case of two interacting chromophores there are at least two non-vanishing SVs of the transition density matrix.[14] This static electron correlation in the Frenkel exciton has been related to the fact that the *electron* and *hole* are always on one molecule together.[10] Furthermore, it was observed that during exciplex formation, this correlation disappeared leading to a homogeneous strongly stabilized state.[10,61,62]

NTOs are very convenient for visualizing individual excitations. However, their downside is that in cases where a large number of excitations are of interest, a correspondingly large set of NTOs has to be constructed. In such cases, it is sometimes possible to resort to the simple Hartree-Fock orbitals. However, these may be badly resolved (e.g., in the case of large basis sets several diffuse MOs may appear before the first π^*-orbital). In order to have a more well defined set of orbitals, which is specifically adapted to the set of excitations of interest, we suggest the use of SA-NTOs. For this purpose, we compute the summed *hole*

$$\bar{\mathbf{D}}_H = \sum_{I=1}^{N} \tilde{\mathbf{D}}^{0I} \tilde{\mathbf{D}}^{0I,\mathrm{T}} \tag{60}$$

and *particle* (or *electron*)

$$\bar{\mathbf{D}}_E = \sum_{I=1}^{N} \tilde{\mathbf{D}}^{0I,\mathrm{T}} \tilde{\mathbf{D}}^{0I} \tag{61}$$

density matrices over a set of N states. These are individually diagonalized

$$\bar{\mathbf{U}}^{\mathrm{T}}\bar{\mathbf{D}}_H\bar{\mathbf{U}} = \mathrm{diag}(\bar{\lambda}_{1,H}, \bar{\lambda}_{2,H}, \ldots), \tag{62}$$

$$\bar{\mathbf{V}}^{\mathrm{T}}\bar{\mathbf{D}}_E\bar{\mathbf{V}} = \mathrm{diag}(\bar{\lambda}_{1,E}, \bar{\lambda}_{2,E}, \ldots), \tag{63}$$

yielding the MO-coefficients ($\bar{\mathbf{U}}$) of the state-averaged *hole* NTOs ($\bar{\psi}_{i,H}$), as well as *particle* NTOs ($\bar{\mathbf{V}}$, $\bar{\psi}_{i,E}$). Note that in general $\bar{\lambda}_{i,H} \neq \bar{\lambda}_{i,E}$, and that these numbers are determined individually by the number of occupied and virtual orbitals involved. To give an efficient representation of the excitation in the SA-NTO basis, the individual transition density matrices are expressed according to

$$\mathbf{X}^{0I} = \bar{\mathbf{U}}^{\mathrm{T}}\tilde{\mathbf{D}}^{0I}\bar{\mathbf{V}}. \tag{64}$$

In general, the $\mathbf{X}^{0I}$ matrix possesses only a few elements, which differ significantly from zero, and may be used as a compact representation of a one-particle excited state. In the case of $N = 1$, the $\mathbf{X}^{0I}$ matrix is of course just the diagonal matrix containing the $\sqrt{\lambda_i}$.

VI. DIFFERENCE DENSITY MATRICES

Another group of analysis methods is based on the difference density matrix

$$\Delta^{0I}(r, r') = \gamma^{II}(r, r') - \gamma^{00}(r, r'). \tag{65}$$

One trivial possibility is to plot the difference density, which is simply the difference between the state densities

$$\begin{aligned}\rho_{\Delta}^{0I}(r) &= \Delta^{0I}(r, r) = \gamma^{II}(r, r) - \gamma^{00}(r, r)\\ &= \rho^{II}(r) - \rho^{00}(r).\end{aligned} \tag{66}$$

However, in many cases the difference density is a complicated function with intricate nodal surfaces[9] and just as for the transition density the integral over all space vanishes

$$\int \rho_{\Delta}^{0I}(r)dr = 0. \tag{67}$$

A. Attachment and detachment densities

To obtain a more meaningful quantity, it was suggested to divide the difference density into individual attachment and detachment components.[9] For this purpose, one considers the matrix representation (again in an orthonormal orbital basis)

$$\mathbf{\Delta}^{0I} = \tilde{\mathbf{D}}^{II} - \tilde{\mathbf{D}}^{00} \tag{68}$$

and diagonalizes it

$$\mathbf{W}^{\mathrm{T}}\mathbf{\Delta}^{0I}\mathbf{W} = \mathrm{diag}(\kappa_1, \kappa_2, \ldots). \tag{69}$$

The detachment density is constructed by only considering the negative eigenvalues

$$d_i = \min(\kappa_i, 0) \tag{70}$$

and a back-transformation to the initial orbital basis

$$\mathbf{D}_D = \mathbf{W}\mathrm{diag}(d_1, d_2, \ldots)\mathbf{W}^{\mathrm{T}}. \tag{71}$$

In an analogous fashion, the attachment density is constructed from the positive eigenvalues

$$a_i = \max(\kappa_i, 0) \tag{72}$$

and a back-transformation

$$\mathbf{D}_A = \mathbf{W}\mathrm{diag}(a_1, a_2, \ldots)\mathbf{W}^{\mathrm{T}}. \tag{73}$$

Using this convention, the matrix $\mathbf{D}_D$ ($\mathbf{D}_A$) is negative (positive) semi-definite, which results in the fact that the corresponding density is lesser (greater) or equal to zero at every point in space. The integrals over all space give the "promotion numbers" $p_D = \mathrm{Tr}(\mathbf{D}_D) = \sum_i d_i$ and $p_A = \mathrm{Tr}(\mathbf{D}_A) = \sum_i a_i$, which can be seen as the numbers of detached and attached electrons, respectively. In the case of an excitation, which does not involve gain or loss of electrons it holds that $-p_D = p_A$, and we will use the symbol p to denote this value. In the case of CIS $p = 1$, but already for a relaxed CIS density $p > 1$.[9] In general, we found in all cases using correlated wavefunction models that $p > 1$.[21] Two distinct reasons for a rise in the promotion number were identified: double excitation character and orbital relaxation effects.

B. Population analysis

Following the ideas presented in Ref. 38, a population analysis of the attachment and detachment densities was implemented as well. This allows to partition these densities into contributions from individual atoms. Here, we use the symbol $p_{\mathrm{D}}(A)$ for the detachment population of atom A and $p_{\mathrm{A}}(A)$ for the attachment population. Per convention $p_{\mathrm{D}}(A)$ is greater or equal to zero, as it describes the positive "hole," and conversely $p_{\mathrm{A}}(A) \leq 0$. The sum of these two populations amounts to the total shift of charge on atom A, i.e.,

$$p_{\mathrm{D}}(A) + p_{\mathrm{A}}(A) = c^I(A) - c^0(A). \tag{74}$$

C. Natural difference orbitals

In light of the above analyses of state and transition densities, it also appears of interest to visualize the eigenvectors of $\mathbf{\Delta}^{0I}$, as given by the $\mathbf{W}$ matrix (see also Ref. 63). The resulting orbitals will be termed NDOs. NDOs with negative (positive) eigenvalues describe the detachment (attachment) process. The sum over all such NDOs squared and multiplied with the respective eigenvalues yields the detachment (attachment) density, similar to Eqs. (57) and (58). In this sense, NDOs provide a decomposition of the attachment/detachment densities, which is especially informative in cases where $p \gg 1$. Examples in Paper II[21] show that the NDOs of singly excited states may be divided into two classes: (i) primary excitation components, which are also visible in the NTO representation and (ii) secondary contributions, which are at first sight counterintuitive but can be identified with orbital relaxation effects.

In analogy to the $\mathrm{PR}_{\mathrm{NTO}}$ value (Eq. (59)), we again define and compute measures that determine how many relevant

NDOs there are: the detachment participation ratio

$$\mathrm{PR}_D = \frac{p_D^2}{\sum_i d_i^2} \tag{75}$$

and the attachment participation ratio

$$\mathrm{PR}_A = \frac{p_A^2}{\sum_i a_i^2}. \tag{76}$$

VII. COMPARISON BETWEEN METHODS

It is interesting to note that in the case of CIS (and related models) all three analysis methods produce the same transformation matrices, i.e., if degenerate subspaces are appropriately resolved,[64] it follows that $\mathbf{T} = \mathbf{U} = \mathbf{V} = \mathbf{W}$. This is apparent, since it has been shown that for CIS NTOs and NOs,[15] as well as NTOs and NDOs[9] are equivalent (see also Refs. 43 and 55). The eigenvalues of NOs and NTOs (in a spin-orbital basis) are related as follows:[15]

$$n_i = \begin{cases} 1-\lambda_i : & i \le n_{\mathrm{occ}} \\ \lambda_i : & n_{\mathrm{occ}} \le i \le 2n_{\mathrm{occ}} \\ 0 : & \text{else} \end{cases}, \tag{77}$$

where n_{occ} denotes the number of occupied orbitals. For NTOs and NDOs, it simply holds that

$$-d_i = a_i = \lambda_i \tag{78}$$

for all non-vanishing λ_i. Furthermore, the CIS vector is equivalent to the transition density matrix (Eq. (40)), which means that also the direct wavefunction analysis contains this information. However, there is a decisive difference between these analysis methods, which may already be understood at the CIS level. NTOs are constructed as pairs of virtual and occupied orbitals (or *electron-hole* pairs). By contrast, NOs describe individual unpaired electrons while NDOs refer to independent attachment/detachment contributions. Whenever $\mathrm{PR}_{\mathrm{NTO}} > 1$ (i.e., the CIS excited state cannot be described by a single configuration) it is necessary to connect the individual *hole* and *electron* contributions to obtain a complete description of the excitation. Such a connection is naturally present in the 1TDM, explaining the advantage of its use for analysis purposes.

Once correlated methods are used, the situation becomes more complicated and differences between NOs, NTOs, and NDOs arise, which may give insight into various many-particle effects. As one example, the NOs and NTOs of an excited state may differ due to dynamic electron correlation, which is already visible in the ground state. Moreover, two distinct reasons for discrepancies between NDOs and NTOs can be identified and will be discussed in detail in Paper II.[21] First, differences may arise from doubly excited configurations, which are not covered by the 1TDM. Second, the NDOs may contain non-intuitive contributions deriving from orbital relaxation effects, a phenomenon, which has received almost no attention in the literature so far.[63]

VIII. ADC IMPLEMENTATION

The ADC scheme constitutes an approach for the construction of excited state methods based on the framework of many-body Green's functions.[4] It involves the perturbation expansion of the polarization propagator (Eq. (36)) yielding a series of methods which can be classified according to their order in perturbation theory.

For each method, an approximate matrix representation of the Hamiltonian is derived in terms of an orthogonal basis of intermediate states (IS) $|\tilde{\Phi}_K\rangle$[65]

$$M_{KL} = \langle \tilde{\Phi}_K | \hat{H} - E^0 | \tilde{\Phi}_L \rangle. \tag{79}$$

Intermediate *electron-hole* amplitudes

$$f_{pq,K} = \langle \tilde{\Phi}_K | \hat{a}_p^\dagger \hat{a}_q | \Psi^0 \rangle \tag{80}$$

and intermediate transition densities

$$B_{pq,KL} = \langle \tilde{\Phi}_K | \hat{a}_p^\dagger \hat{a}_q | \tilde{\Phi}_L \rangle \tag{81}$$

are obtained, as well. Detailed equations for these quantities for methods up to third order can be found elsewhere.[4,66–68]

Diagonalization of the Hamiltonian matrix $\mathbf{M}$ yields the excitation energies as eigenvalues. The respective eigenvectors $\mathbf{y}^I$ provide access to the excited state wave functions via the relation

$$|\Psi^I\rangle = \sum_K y_K^I |\tilde{\Phi}_K\rangle. \tag{82}$$

A great advantage of the intermediate state representation is that the 1TDMs can be directly obtained by combining the eigenvectors with the intermediate *electron-hole* amplitudes

$$\begin{aligned} D_{pq}^{0I} &= \langle \Psi^0 | \hat{a}_p^\dagger \hat{a}_q | \Psi^I \rangle = \sum_K \langle \Psi^0 | \hat{a}_p^\dagger \hat{a}_q | \tilde{\Phi}_K \rangle y_K^I \\ &= \sum_K f_{pq,K}^\dagger y_K^I = \mathbf{f}_{pq}^\dagger \mathbf{y}^I. \end{aligned} \tag{83}$$

Similarly, the 1DMs can be directly computed from the intermediate transition densities

$$D_{pq}^{II} = \sum_{KL} y_K^I B_{pq,KL} y_L^I + D_{pq}^{00} = \mathbf{y}^{I\dagger} \mathbf{B}_{pq} \mathbf{y} + D_{pq}^{00}, \tag{84}$$

where D_{pq}^{00} is the ground state density at the respective level of perturbation theory.

The above described analysis tools have been implemented using the 1DMs and 1TDMs in the ADC framework. They are currently available as part of the ADC module of the Q-Chem program package[68–70] and allow for the analysis of density matrices resulting from calculations using the ADC(1), ADC(2)-s, ADC(2)-x, and ADC(3) models. The code is written in a modular fashion to make it transferable to other wavefunction models or quantum chemical programs in the future.

IX. CONCLUSIONS

A number of methods for the visual and numerical analysis of electronic excitations have been reviewed and new related approaches have been suggested. For this purpose, a

formalism based on density matrices is used, which are well-defined quantities independent of the wavefunction model and are naturally connected to physical observables through operator matrix elements. Aside from the presentation of the equations used, their physical interpretation has been discussed in detail. Furthermore, the implementation of these methods within the ADC module of the Q-Chem program package has been reported. The program code described here will be made available as an independent module to be used for other wavefunction models and with other quantum chemistry codes in the future.

First, state density matrices were considered. These give rise to some of the most common concepts in quantum chemistry: (i) density plots and population analyses, which can be used to visualize and quantify average electronic positions, and (ii) NOs, which are a convenient way to analyze unpaired electrons. Second, 1TDMs were discussed. It was shown how the 1TDM can be used to provide a compact description of the excitation by a decomposition into NTOs and the *hole* and *particle* densities composed of them. We extended these ideas with the concept of state-averaged NTOs, which constitute a set of orbitals suited for the simultaneous visualization of a number of excited states. Furthermore, it was explained how the 1TDM can be exploited to analyze charge resonance effects and *electron-hole* correlations as defined within many-body Green's function theory. Third, difference density matrices were considered. These are used to define the attachment/detachment densities, which provide a compact representation of electron rearrangements. Additionally, we suggest plotting the eigenvectors of the difference density matrix, the NDOs, to decompose the attachment/detachment densities into individual contributions, which may be used to visualize orbital relaxation effects.

We discussed similarities and differences between these methods, showing that in the case of CIS all methods yield essentially the same outcome, except for *electron-hole* correlations, which are explicitly coded only in the transition density matrix. In the case of many-particle methods, the NOs, NTOs, and NDOs differ and provide a view at different correlation and relaxation effects.

In Paper II,[21] a diverse set of example applications will follow. These will illustrate many of the described concepts and show that the tools described do not only allow to automatize the analysis procedures but, more importantly, reveal new information which cannot be recovered in the simple orbital excitation picture. In particular, the significance of orbital relaxation and *electron-hole* correlation effects will be illuminated. In conclusion, we hope that this work will spur new interest in the analysis of excited state wavefunctions.

ACKNOWLEDGMENTS

F.P. gratefully acknowledges discussions with H. Lischka, I. Burghardt, and A. Krylov pertaining to different aspects of the presented material. F.P. is a recipient of a fellowship for postdoctoral researchers by the Alexander von Humboldt foundation.

APPENDIX A: GENERALIZED BASIS SET TRANSFORMATION

The purpose of this appendix is to give a simple proof for Eq. (56), and similarly Eqs. (29), (57), and (58). We show that given a function

$$\gamma^{IJ}(r,r') = \sum_{pq} \tilde{D}^{IJ}_{pq}\phi_p(r)\phi_q(r') \tag{A1}$$

and assuming that

$$\tilde{\mathbf{D}}^{IJ} = \mathbf{U}\mathrm{diag}(\sqrt{\lambda_1}, \sqrt{\lambda_2}, \ldots)\mathbf{V}^{\mathrm{T}} \tag{A2}$$

and

$$\psi_i^{IJ}(r) = \sum_p U_{pi}\phi_p(r), \tag{A3}$$

$$\psi_i^{JI}(r) = \sum_p V_{pi}\phi_p(r), \tag{A4}$$

it follows that γ^{IJ} may be expressed in diagonal form

$$\gamma^{IJ}(r,r') = \sum_i \sqrt{\lambda_i}\psi_i^{IJ}(r)\psi_i^{JI}(r'). \tag{A5}$$

Proof: One collects the functions in a column vector

$$\underline{\phi}(r) = \begin{pmatrix} \phi_1(r) \\ \vdots \\ \phi_n(r) \end{pmatrix} \tag{A6}$$

and similarly for $\underline{\psi}^{IJ}(r)$ and $\underline{\psi}^{JI}(r)$. Using this notation Eq. (A3) can be rewritten as

$$\underline{\psi}^{IJ}(r)^{\mathrm{T}} = \underline{\phi}(r)^{\mathrm{T}}\mathbf{U} \tag{A7}$$

and because $\mathbf{U}$ is unitary

$$\underline{\phi}(r) = \mathbf{U}\underline{\psi}^{IJ}(r). \tag{A8}$$

It may be seen in an analogous fashion that

$$\underline{\phi}(r') = \mathbf{V}\underline{\psi}^{JI}(r'). \tag{A9}$$

Using these definitions Eq. (A1) becomes

$$\gamma^{IJ}(r,r') = \underline{\phi}(r)^{\mathrm{T}}\tilde{\mathbf{D}}^{IJ}\underline{\phi}(r'). \tag{A10}$$

Inserting Eqs. (A8), (A2), and (A9) leads to

$$\begin{aligned}\gamma^{IJ}(r,r') &= (\mathbf{U}\underline{\psi}^{IJ}(r))^{\mathrm{T}}\mathbf{U}\,\mathrm{diag}(\sqrt{\lambda_1}, \sqrt{\lambda_2}, \ldots)\mathbf{V}^{\mathrm{T}}\mathbf{V}\underline{\psi}^{JI}(r') \\ &= \underline{\psi}^{IJ}(r)^{\mathrm{T}}\mathrm{diag}(\sqrt{\lambda_1}, \sqrt{\lambda_2}, \ldots)\underline{\psi}^{JI}(r'). \end{aligned} \tag{A11}$$

Equation (A11) is the desired result and may be used immediately to show Eq. (56). The analogous equation for NOs (29) simply follows by setting $J \to I$, $\mathbf{U} \to \mathbf{T}$, $\mathbf{V} \to \mathbf{T}$, and $\sqrt{\lambda_i} \to n_i$. And, of course, the analogous relation holds for NDOs as well.

APPENDIX B: BASIS SET REPRESENTATION OF THE CHARGE TRANSFER NUMBERS

In this section, the Mulliken style analysis of the charge transfer numbers will be given. Starting with the real space

representation of Eq. (49) and inserting Eq. (12) one obtains

$$\begin{aligned}\Omega_{AB} &= \int_A \int_B \gamma^{0I}(r_H, r_E)^2 dr_E dr_H \\ &= \sum_{\mu\nu}\sum_{\xi\zeta} D^{0I}_{\mu\nu} D^{0I}_{\xi\zeta} \int_A \chi_\mu(r_H)\chi_\xi(r_H) dr_H \\ &\quad \times \int_B \chi_\nu(r_E)\chi_\zeta(r_E) dr_E \\ &= \sum_{\mu\nu}\sum_{\xi\zeta} D^{0I}_{\mu\nu} D^{0I}_{\xi\zeta} S^{(A)}_{\mu\xi} S^{(B)}_{\nu\zeta}. \end{aligned} \tag{B1}$$

For the partial overlap integrals, initially defined in Eq. (23), we use the compressed notation

$$S^{(A)}_{\mu\nu} = \frac{1}{2}([\mu \in A] + [\nu \in A]) S_{\mu\nu}, \tag{B2}$$

where the "Iverson bracket" notation is used: $[X]$ is equal to 1 if the statement X is true and 0 otherwise. Using this definition, Eq. (B1) can be reexpressed as

$$\begin{aligned}\Omega_{AB} &= \frac{1}{4}\sum_{\mu\nu}\sum_{\xi\zeta} D^{0I}_{\mu\nu} D^{0I}_{\xi\zeta} S_{\mu\xi}([\mu \in A] + [\xi \in A]) \\ &\quad \times S_{\nu\zeta}([\nu \in B] + [\zeta \in B]) \\ &= \frac{1}{4}\sum_{\mu\nu}\sum_{\xi\zeta} D^{0I}_{\mu\nu} D^{0I}_{\xi\zeta} S_{\mu\xi} S_{\nu\zeta} \\ &\quad \big([\mu \in A][\nu \in B] + [\xi \in A][\nu \in B] \\ &\quad + [\mu \in A][\zeta \in B] + [\xi \in A][\zeta \in B]\big). \end{aligned} \tag{B3}$$

These terms are evaluated by realizing that the full summations can be written as matrix multiplications while the partial summations are kept explicitly

$$\begin{aligned} &= \frac{1}{4}\left(\sum_{\mu\in A}\sum_{\nu\in B} D^{0I}_{\mu\nu}(\mathbf{S}\mathbf{D}^{0I}\mathbf{S})_{\mu\nu} + \sum_{\xi\in A}\sum_{\nu\in B}(\mathbf{S}\mathbf{D}^{0I})_{\xi\nu}(\mathbf{D}^{0I}\mathbf{S})_{\xi\nu}\right. \\ &\quad + \sum_{\mu\in A}\sum_{\zeta\in B}(\mathbf{S}\mathbf{D}^{0I})_{\mu\zeta}(\mathbf{D}^{0I}\mathbf{S})_{\mu\zeta} + \sum_{\xi\in A}\sum_{\zeta\in B}(\mathbf{S}\mathbf{D}^{0I}\mathbf{S})_{\xi\zeta} D^{0I}_{\xi\zeta}) \\ &= \frac{1}{2}\left.\sum_{\mu\in A}\sum_{\nu\in B}(D^{0I}_{\mu\nu}(\mathbf{S}\mathbf{D}^{0I}\mathbf{S})_{\mu\nu} + (\mathbf{S}\mathbf{D}^{0I})_{\mu\nu}(\mathbf{D}^{0I}\mathbf{S})_{\mu\nu}\right). \end{aligned} \tag{B4}$$

[1] A. Dreuw and M. Head-Gordon, Chem. Rev. **105**, 4009 (2005).
[2] F. Plasser, M. Barbatti, A. J. A. Aquino, and H. Lischka, Theor. Chem. Acc. **131**, 1073 (2012).
[3] L. González, D. Escudero, and L. Serrano-Andrés, ChemPhysChem **13**, 28 (2012).
[4] J. Schirmer, Phys. Rev. A **26**, 2395 (1982).
[5] P.-O. Lowdin, Phys. Rev. **97**, 1474 (1955).
[6] A. V. Luzanov, A. A. Sukhorukov, and V. E. Umanskii, Theor. Exp. Chem. **10**, 354 (1976).
[7] R. L. Martin, J. Chem. Phys. **118**, 4775 (2003).
[8] I. Mayer, Chem. Phys. Lett. **437**, 284 (2007).
[9] M. Head-Gordon, A. Grana, D. Maurice, and C. White, J. Phys. Chem. **99**, 14261 (1995).
[10] F. Plasser and H. Lischka, J. Chem. Theory Comput. **8**, 2777 (2012).
[11] A. L. L. East and E. C. Lim, J. Chem. Phys. **113**, 8981 (2000).
[12] S. Tretiak and S. Mukamel, Chem. Rev. **102**, 3171 (2002).
[13] A. V. Luzanov and O. A. Zhikol, Int. J. Quantum Chem. **110**, 902 (2010).
[14] I. Mayer, Chem. Phys. Lett. **443**, 420 (2007).
[15] P. R. Surján, Chem. Phys. Lett. **439**, 393 (2007).
[16] F. Plasser, A. J. A. Aquino, W. L. Hase, and H. Lischka, J. Phys. Chem. A **116**, 11151 (2012).
[17] A. N. Panda, F. Plasser, A. J. A. Aquino, I. Burghardt, and H. Lischka, J. Phys. Chem. A **117**, 2181 (2013).
[18] D. Balamurugan, A. J. A. Aquino, F. de Dios, L. Flores, H. Lischka, and M. S. Cheung, J. Phys. Chem. B **117**, 12065 (2013).
[19] R. Binder, J. Wahl, S. Römer, and I. Burghardt, Faraday Discuss. **163**, 205 (2013).
[20] L. Blancafort and A. A. Voityuk, J. Chem. Phys. **140**, 095102 (2014).
[21] F. Plasser, M. Wormit, and A. Dreuw, J. Chem. Phys. **141**, 024107 (2014).
[22] J.-L. Brédas, J. Cornil, D. Beljonne, D. A. dos Santos, and Z. Shuai, Acc. Chem. Res. **32**, 267 (1999).
[23] N. Kirova, Polym. Int. **57**, 678 (2008).
[24] M. Rohlfing and S. G. Louie, Phys. Rev. Lett. **82**, 1959 (1999).
[25] J.-W. van der Horst, P. A. Bobbert, M. A. J. Michels, G. Brocks, and P. J. Kelly, Phys. Rev. Lett. **83**, 4413 (1999).
[26] T. G. Pedersen and T. B. Lynge, Comput. Mater. Sci. **27**, 123 (2003).
[27] T. G. Pedersen, P. M. Johansen, and H. C. Pedersen, Phys. Rev. B **61**, 10504 (2000).
[28] W. Barford and N. Paiboonvorachat, J. Chem. Phys. **129**, 164716 (2008).
[29] C. Wu, S. V. Malinin, S. Tretiak, and V. Y. Chernyak, J. Chem. Phys. **129**, 174111 (2008).
[30] W. Barford and D. Trembath, Phys. Rev. B **80**, 165418 (2009).
[31] T. M. Clarke and J. R. Durrant, Chem. Rev. **110**, 6736 (2010).
[32] Z. L. Cai, K. Sendt, and J. R. Reimers, J. Chem. Phys. **117**, 5543 (2002).
[33] S. Tretiak, K. Igumenshchev, and V. Chernyak, Phys. Rev. B **71**, 033201 (2005).
[34] V. Lukes, A. J. A. Aquino, H. Lischka, and H.-F. Kauffmann, J. Phys. Chem. B **111**, 7954 (2007).
[35] D. Lumpi, E. Horkel, F. Plasser, H. Lischka, and J. Fröhlich, ChemPhysChem **14**, 1016 (2013).
[36] N. Kuritz, T. Stein, R. Baer, and L. Kronik, J. Chem. Theory Comput. **7**, 2408 (2011).
[37] A. Dreuw and M. Head-Gordon, J. Am. Chem. Soc. **126**, 4007 (2004).
[38] R. Richard and J. Herbert, J. Chem. Theory Comput. **7**, 1296 (2011).
[39] G. D. Scholes and K. P. Ghiggino, J. Phys. Chem. **98**, 4580 (1994).
[40] X. Feng, A. V. Luzanov, and A. I. Krylov, J. Phys. Chem. Lett. **4**, 3845 (2013).
[41] In the general case, one cannot make a distinction between occupied and virtual orbitals, and therefore all the sums go over the whole orbital basis.
[42] R. J. Bartlett and M. Musiał, Rev. Mod. Phys. **79**, 291 (2007).
[43] E. Batista and R. Martin, "Natural transition orbitals," *Encyclopedia of Computational Chemistry* (John Wiley and Sons, Inc., 2004).
[44] F. Plasser, "Quantum mechanical simulations of defect dynamics in DNA and model systems," Ph.D. thesis, University of Vienna, 2012.
[45] J. Skolnik and D. Mazziotti, Phys. Rev. A **88**, 032517 (2013).
[46] R. S. Mulliken, J. Chem. Phys. **23**, 1833 (1955).
[47] E. Ramos-Cordoba and P. Salvador, J. Chem. Theory Comput. **10**, 634 (2014).
[48] K. Takatsuka, T. Fueno, and K. Yamaguchi, Theor. Chim. Acta **48**, 175 (1978).
[49] M. Head-Gordon, Chem. Phys. Lett. **372**, 508 (2003).
[50] F. Plasser, H. Pašalić, M. H. Gerzabek, F. Libisch, R. Reiter, J. Burgdörfer, T. Müller, R. Shepard, and H. Lischka, Angew. Chem., Int. Ed. **52**, 2581 (2013).
[51] Z. Cui, H. Lischka, T. Müller, F. Plasser, and M. Kertesz, ChemPhysChem **15**, 165 (2014).
[52] J. Rissler, H. Bässler, F. Gebhard, and P. Schwerdtfeger, Phys. Rev. B **64**, 045122 (2001).
[53] G. Strinati, Phys. Rev. B **29**, 5718 (1984).
[54] M. Rohlfing and S. Louie, Phys. Rev. B **62**, 4927 (2000).
[55] A. Luzanov and O. Zhikol, in *Practical Aspects of Computational Chemistry I*, edited by J. Leszczynski and M. K. Shukla (Springer, Netherlands, 2012), pp. 415–449.
[56] A. Voityuk, Photochem. Photobiol. Sci. **12**, 1303 (2013).
[57] A. V. Luzanov and O. V. Prezhdo, Int. J. Quantum Chem. **102**, 582 (2005).
[58] I. Mayer, Chem. Phys. Lett. **97**, 270 (1983).
[59] M. Sun, P. Kjellberg, W. J. Beenken, and T. Pullerits, Chem. Phys. **327**, 474 (2006).
[60] I. G. Scheblykin, A. Yartsev, T. Pullerits, V. Gulbinas, and V. Sundström, J. Phys. Chem. B **111**, 6303 (2007).

[61]F. Plasser and H. Lischka, Photochem. Photobiol. Sci. **12**, 1440 (2013).
[62]F. Plasser, A. Aquino, H. Lischka, and D. Nachtigallova, in *Photoinduced Phenomena in Nucleic Acids*, edited by M. Barbatti, A. C. Borin, and S. Ullrich (Springer, 2014).
[63]A. D. Dutoi, L. S. Cederbaum, M. Wormit, J. H. Starcke, and A. Dreuw, J. Chem. Phys. **132**, 144302 (2010).
[64]For this formal statement, it is assumed that all matrices go over the whole orbital space, which means that potentially a large number of zero eigenvalues are present.
[65]J. Schirmer, Phys. Rev. A **43**, 4647 (1991).
[66]A. B. Trofimov, G. Stelter, and J. Schirmer, J. Chem. Phys. **111**, 9982 (1999).
[67]J. Schirmer and A. B. Trofimov, J. Chem. Phys. **120**, 11449 (2004).
[68]M. Wormit, D. R. Rehn, P. H. Harbach, J. Wenzel, C. M. Krauter, E. Epifanovsky, and A. Dreuw, Mol. Phys. **112**, 774 (2014).
[69]Y. Shao, L. F. Molnar, Y. Jung, J. Kussmann, C. Ochsenfeld, S. T. Brown, A. T. Gilbert, L. V. Slipchenko, S. V. Levchenko, D. P. O'Neill, R. A. DiStasio, Jr., R. C. Lochan, T. Wang, G. J. Beran, N. A. Besley, J. M. Herbert, C. Yeh Lin, T. Van Voorhis, S. Hung Chien, A. Sodt, R. P. Steele, V. A. Rassolov, P. E. Maslen, P. P. Korambath, R. D. Adamson, B. Austin, J. Baker, E. F. C. Byrd, H. Dachsel, R. J. Doerksen, A. Dreuw, B. D. Dunietz, A. D. Dutoi, T. R. Furlani, S. R. Gwaltney, A. Heyden, S. Hirata, C.-P. Hsu, G. Kedziora, R. Z. Khalliulin, P. Klunzinger, A. M. Lee, M. S. Lee, W. Liang, I. Lotan, N. Nair, B. Peters, E. I. Proynov, P. A. Pieniazek, Y. Min Rhee, J. Ritchie, E. Rosta, C. David Sherrill, A. C. Simmonett, J. E. Subotnik, H. Lee Woodcock III, W. Zhang, A. T. Bell, A. K. Chakraborty, D. M. Chipman, F. J. Keil, A. Warshel, W. J. Hehre, H. F. Schaefer III, J. Kong, A. I. Krylov, P. M. W. Gill, and M. Head-Gordon, Phys. Chem. Chem. Phys. **8**, 3172 (2006).
[70]A. I. Krylov and P. M. W. Gill, WIREs: Comput. Mol. Sci. **3**, 317 (2013).